PRESSURELESS SINTERING OF ZIRCONIUM DIBORIDE

OBTAINED BY COMBUSTION SYNTHESIS

GABRIEL LLAUSAS

Master's Program in Mechanical Engineering

Approved:

Evgeny Shafirovich, Ph.D., Chair

Arturo Bronson, Ph.D.

David Roberson, Ph.D.

Stephen Crites, Ph.D.
Dean of the Graduate School

Dedication

Me gustaría dedicar esta tesis a mis padres, por su apoyo incondicional, a mis hermanos, abuelos, tíos y primos. A mis amigos y a todos aquellos que me han apoyado a través de los años.

PRESSURELESS SINTERING OF ZIRCONIUM DIBORIDE OBTAINED BY COMBUSTION SYNTHESIS

By

GABRIEL LLAUSAS, B.S

THESIS

Presented to the faculty of the graduate school of

The University of Texas at El Paso

in partial fulfillment

of the requirements

for the degree of

MASTER OF SCIENCE

Department of Mechanical Engineering

THE UNIVERSITY OF TEXAS AT EL PASO

May 2019

Acknowledgements

I would like to thank my advisor Dr. Evgeny Shafirovich for providing mentoring and the opportunity to be involved in his research activities. Also, I would like to thank my thesis committee members, Dr. Arturo Bronson, and Dr. David Roberson, for spending the time to read this document. I would like to thank my lab mates Sergio Cordova, Alan Esparza, Robert Ferguson, Ralph Vargas, Edgar Maguregui, and Reina Treviño for their help. Lastly, to the National Energy Technology Laboratory of the U.S. Department of Energy for funding this research under award DE-FE002633.

Abstract

Magnetohydrodynamic (MHD) direct power generation has the potential to significantly increase the thermal efficiency of coal fired power plants. Materials for MHD electrodes should have high melting points, high electrical and thermal conductivities, and excellent thermal shock and corrosion resistance. Zirconium diboride (ZrB_2), which belongs to the class of ultra-high temperature ceramics (UHTC), is a promising material for this application. Mechanically activated self-propagating high-temperature synthesis (MASHS) is an attractive method for its fabrication. Previous studies have shown that zirconium diboride can be fabricated from inexpensive oxides of zirconium and boron (ZrO_2 and B_2O_3) using magnesium as a reducing agent and sodium chloride as an inert diluent. It was determined that for the highest conversion of ZrO_2 and B_2O_3 to ZrB_2, the concentration of Mg in the ZrO_2/B_2O_3/Mg/NaCl mixture should be higher by 20% than the stoichiometric one and the mixture should include 30 wt% NaCl. However, 100% conversion was not achieved and the obtained product was a loose powder. In the present work, pressureless sintering of ZrB_2 obtained by magnesiothermic MASHS was studied for its purification and densification. The effects of additives (boron carbide and molybdenum silicide) and operating parameters (milling time and initial density) on the density and composition of the final product were investigated. The experiments have confirmed the effectiveness of both additives in converting the remaining oxides to ZrB_2. It has been shown that milling, pressing, and adding boron carbide are needed for enhancing the sinterability of zirconium diboride.

Table of Contents

List of Figures

Chapter 1: Introduction

1.1 Electrodes of Magnetohydrodynamic Generators

Magnetohydrodynamic (MHD) direct power extraction can potentially increase the efficiency of coal-fired power plants. MHD power generators have no moving parts and metal conductors are replaced by ionized gas (plasma), hence they have high thermal efficiency [1]. MHD power generation is governed by Faraday's law of electromagnetic induction. The high velocity flow of conducting plasma through an applied magnetic field generates a voltage across the electrodes [1,2]. Unlike conventional turbine-based power plants, MHD generators directly convert thermal energy to electricity, without an intermediate generation of mechanical shaft power [2].

Unfortunately, there is a lack of suitable materials for MHD power generation [1,2]. One of the major problems is the development of electrodes capable of withstanding long operational periods [2]. Because of severe operating conditions, the electrodes must have a high melting point, high resistance to thermal shock and oxidation, high electrical conductivity, high thermal conductivity, good thermionic emission, high mechanical stability (creep resistance) and excellent corrosion resistance [1-4]. One promising material for MHD electrodes is zirconium diboride [5].

1.2 Magnesiothermic SHS of Zirconium Diboride

There are several methods for fabrication of zirconium diboride. Carbothermic and borothermic reduction of ZrO_2 are popular methods for its synthesis. However, these methods require long milling times and high-temperature furnaces. Magnesiothermic reduction of

$ZrO_2/B_2O_3/Mg$ mixtures can be performed as a combustion process, which requires low energy input and short milling times compared to borothermic and carbothermic reduction. This process can be performed as the so-called self-propagating high-temperature synthesis (SHS), where the combustion wave propagates over the mixture upon ignition. Prior experiments, however, have revealed incomplete conversion of ZrO_2 to ZrB_2 in magnesiothermic SHS [6]. Recently, studies for optimizing the experimental parameters have been conducted where the optimal conditions were determined for the highest conversion [6]. Oxygen content in the obtained products was below 4%. However, full elimination of oxygen from the product would be desirable.

1.3 Sintering of Zirconium Diboride

SHS products are porous and require densification. Sintering is an attractive densification method of materials. Zirconium diboride is thought to have low intrinsic sinterability due to its covalent bonds, presence of surface oxides (ZrO_2 and B_2O_3), and low bulk and grain boundary diffusivities. In order to be sintered, it requires high temperatures (at least 1900 °C) and pressures of 20-30 MPa [7]. However, hot-press sintering is limited to simple geometries and moderate sizes. Spark plasma sintering has also produced high-density zirconium diboride [5,8-10], but it also requires simple geometries. Pressureless sintering of zirconium diboride has been explored in recent studies because it does not involve high pressures and can produce near net shape items [7,8,11-14].

Most recent studies focused on the use of additives acting as reducing agents [8,11,12] and milling [12,13] of powders to promote densification. The former aids in the reduction of oxide layers on the surface of grain boundaries, which promote grain growth, inhibiting densification. The latter focuses on reducing the surface energy, which leads to pore reduction. Both these

factors have an effect on final density. Some additives can also reduce the remaining oxides (in other words, eliminate oxygen impurity), leading to a higher conversion to the boride.

1.4 Objective

The objective of this present work was to investigate factors that may improve pressureless sintering of zirconium diboride obtained from zirconia and boron oxide by magnesiothermic MASHS. Specifically, the effects of additives and milling on the densification and purification of the product were studied.

Chapter 2: Literature Review

2.1 Zirconium Diboride

Metal borides possess attractive properties to serve as refractory alloys for the development of high-temperature ceramics and metalloceramics [15]. Zirconium diboride has a relatively low density (6.08 g/cm^3) and high electical and thermal conductivities [16]. It has a hexagonal crystal structure. Its high melting point (3246 °C), high Vickers' hardness (23 GPa), and high four-point flexural strength (565 MPa) can be attributed to its highly covalent nature [15]. These properties make it attractive to serve as a material for MHD electrodes and other high-temperature applications with corrosive environments [5,17,12].

2.2 Sintering of Zirconium Diboride

The sintering behavior of ceramics is largely influenced by factors such as temperature, heating rate, and holding time. It has been widely observed that density is a function of sintering temperature [10,12].

Different sintering methods for zirconium diboride have been studied, such as hot pressing, spark plasma sintering, and pressureless sintering. Because of its covalent bonds, presence of surface oxides, and low bulk and grain boundary diffusivities, zirconium diboride is thought to have low intrinsic sinterability [7]. Densification typically requires temperatures of 1900 °C or higher, as well as applied pressures of 20-30 MPa. Hot pressing and spark plasma sintering are effective methods for densification of zirconium diboride, but these techniques are limited to simple geometries as well as moderate sizes and require substantial diamond machining, raising processing cost, which has led to exploring advances in pressureless sintering [7].

Previous studies have shown that the addition of additives and milling times can enhance the sinterability of ZrB_2. Due to its high melting point, zirconium diboride requires pressure-assisted methods of densification at temperatures of 1900 °C or higher without additives [7]. This has led to research in the use of additives for enhancing the sinterability of ZrB_2 [21].

2.2.1 Hot Press Sintering of Zirconium Diboride

Hot press sintering experiments have reported high densities at temperatures higher than 1900 °C [7,10]. Molybdenum silicide [8,9], silicon carbide [18] and boron carbide[19] have been studied as potential additives for hot pressing of zirconium diboride as enhancers of densification. High-density samples (98-99%) were obtained with 15 or 20 vol% of $MoSi_2$ [8].

For experiments studying hot pressing involving ZrB_2-SiC composites, the effect of sintering temperatures was studied [18]. Experiments varied temperatures from 1850 – 2050 °C with increments of 100 °C, with three different holding times (45, 90 and 180 min) at the highest temperature of 2050 °C. Results reported relative densities of 97% and above.

For experiments using B_4C [19] as an additive, relatively high densities (~97%) were obtained by adding 1.68 wt% B_4C at sintering temperatures of 2000 °C. However, fracture surfaces of samples revealed pores.

2.2.2 Spark Plasma Sintering of Zirconium Diboride

Spark plasma sintering (SPS) is one of the most recent sintering techniques being explored for the densification of ceramic materials [10]. Although sharing similarities, spark plasma sintering and hot press sintering are two different techniques. Hot pressing uses indirect heating with applied pressures. Spark plasma sintering uses an applied electric field in order to

heat the pressing die and compact [10]. An advantage of this method is that it enhances the sinterability of ceramics as a result of simultaneously applying a uniaxial load with a direct or pulsed electrical current to a powder compact.

Previous studies have been successful at achieving high-density zirconium diboride by SPS. Near-fully dense compacts have been obtained through sintering at 1900 °C for 3 min, with heating rates greater than 200 °C. Compared to hot pressing, SPS times are significantly shorter.

The introduction of additives for densification during SPS has resulted in lowering sintering temperatures while still obtaining near-fully dense compacts. In one study with a sample composition of ZrB_2 with 15 vol% $MoSi_2$, a relative density of about 97% was obtained at a maximum sintering temperature of 1750 °C [5]. In the same work, the addition of SiC along with ZrC as sintering aids was studied. For these additions, samples reached a relative density of 99%, but a much higher temperature was required (2100 °C). Lastly, in a study on the effect of B_4C as an additive for heat treated (prior to sintering) powder systems, samples of ZrB_2 with as little as 0.25 wt% B_4C reached 99% relative density at a temperature of 1900 °C [20].

2.2.3 Pressureless Sintering of Zirconium Diboride

Studies on pressureless sintering of ZrB_2 without additives have shown that density increases at temperatures of up to 2100 °C, but relative densities higher than 78% have been difficult to attain [11]. This has led to the investigation of additive enhanced sintering.

One of the tested additives is molybdenum silicide ($MoSi_2$). Studies have been conducted with varying its concentration from 15 to 20 vol%, temperature from 1800 to 1850 °C, and holding time from 30 to 60 min. Final densities of up to 99% were obtained at the concentration of 20 vol% $MoSi_2$ [8].

Another additive is silicon carbide (SiC). It was used to create ZrB_2-SiC composite ceramics by pressureless sintering. One study initially explored sintering of compositions that included 70 vol% ZrB_2 and 30 vol% SiC at temperatures of 2050 °C and 2100 °C for 3 – 4 h [21]. The highest relative density achieved in these experiments was about 70%. Later experiments have shown that the introduction of 4 wt% B_4C and 7.3 wt% C to these ZrB_2-SiC ceramics for sintering resulted in reaching near full density at a temperature of 2050 °C for 2 h in an argon environment [21].

Boron carbide is a popular additive because of its effectiveness in removing surface oxides [11]. Boron oxide (an oxide impurity of ZrB_2), which has a high vapor pressure in the range of sintering temperatures for ZrB_2, must be removed prior to reaching this range. This can be accomplished through evaporation with a plateau step at temperatures below 1650 °C, using a vacuum pump to maintain pressure of about 0.15 Torr [11,12]. This is advantageous because with increasing the sintering temperature, particle size increases. By this evaporation step, the particle size is not affected.

Mass loss during sintering is inevitable; this is mainly due to the loss of oxygen with gaseous reaction products through the reduction of ZrO_2 (see below). The oxide impurities can be removed by two methods. As mentioned in the previous paragraph, boron oxide can be removed by evaporation, while zirconia can be removed through a chemical reaction [11]. With the addition of boron carbide as a reducing agent, a favorable reaction occurs at temperatures as low as 1428 °C while maintaining a pressure of 0.15 Torr [12,13]. The chemical reaction is as follows:

$$7ZrO_2 + 5B_4C \rightarrow 7ZrB_2 + 3B_2O_3 + 5CO\ (g)$$

The removal of zirconia is critical to increasing density during sintering experiments. The oxygen content in zirconium diboride is primarily in the form of zirconia. It is suggested that the total oxygen content be limited to 5 wt%, otherwise strong reducing agents must be used to promote densification. The reason behind this is the fact that zirconia along with boron oxide promote grain growth and coarsening [22]. This leads to higher porosities after heating and is consistent amongst different sintering methods [7,10,13]. Therefore, the use of additives that act as reducing agents are critical for densification.

In addition to additives, milling is an important precursor for preparation of powders for sintering. The starting particle size can play an important role for the final density. As previously mentioned, the presence of zirconia can lead to grain growth at high temperatures, resulting in high porosity. Large initial particle sizes combined with the possibility of grain growth due to the presence oxides will ultimately have a negative effect on the final density of samples.

Milling decreases the average particle size (thus increasing surface area) of zirconium diboride particles; this related to having surface free energy, which is the driving force for sintering. Therefore, any reduction in particle size results in the enhancement of the sinterability of the powder [12,13].

In conclusion, sintering additives and milling are both necessary for promoting sintering.

2.2.4 Summary of Sintering Methods

Three sintering methods have been reviewed in this section. The following list summarizes advantages and disadvantages of these methods.

1. Hot-press sintering and spark plasma sintering have consistently shown good results in reaching near full density of the samples.

2. Hot-press sintering and spark plasma sintering are constricted to fabrication of simple geometries and moderate sizes, requiring expensive processing.
3. Additives are typically required to enhance sample hot-pressing and spark plasma sintering.
4. Pressureless sintering is a promising method for the densification of zirconium diboride because it does not require high pressures and can produce near net shape items.
5. Powders for pressureless sintering require milling and additives as reducing agents for the elimination of oxides present in zirconium diboride.

Chapter 3: Experimental Procedures

3.1 Sample Preparation

3.1.1 Synthesis of Zirconium Diboride

Zirconium diboride was fabricated by magnesiothermic MASHS following the procedure described in [6]. Specifically, the initial mixture included ZrO_2, B_2O_3, Mg, and NaCl. The composition of the mixture was the stoichiometric mixture of $ZrO_2/B_2O_3/Mg$ with an additional 20% excess Mg and 30 wt% NaCl. Powders were mixed in a 3D inversion kinematics mixer (Fig. 3.1.1) and milled for 5 min in a planetary ball mill (Fritsch Pulverisette 7 Premium Line, Fig. 3.1.2). After milling, powders were pressed into a cylindrical pellet (mass: 4 g, diameter: 13 mm) using a hydraulic press and a trapezoidal die (Across International, Fig 3.1.3).

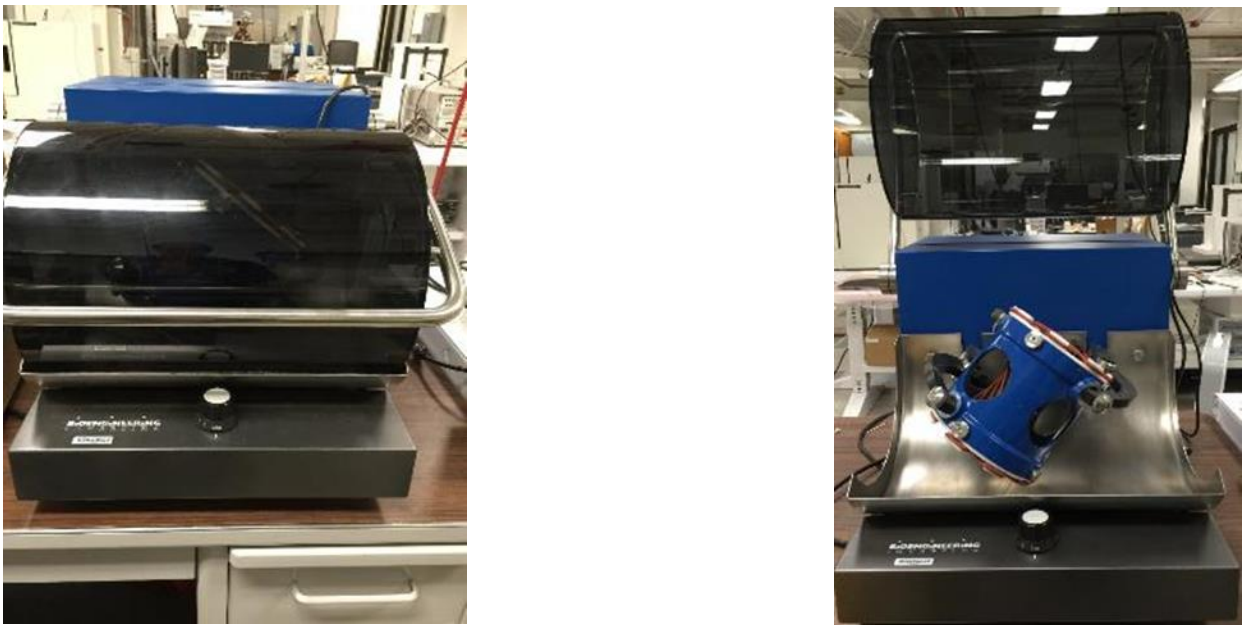

(a) (b)

Figure 3.1.1: Mixer (Inversina 2L, Bioengineering) with (a) closed and (b) open protective shield.

(a) (b)

Figure 3.1.2: Milling equipment: (a) planetary ball mill (Fritsch Pulverisette 7 Premium Line) and (b) milling bowls with purging valves

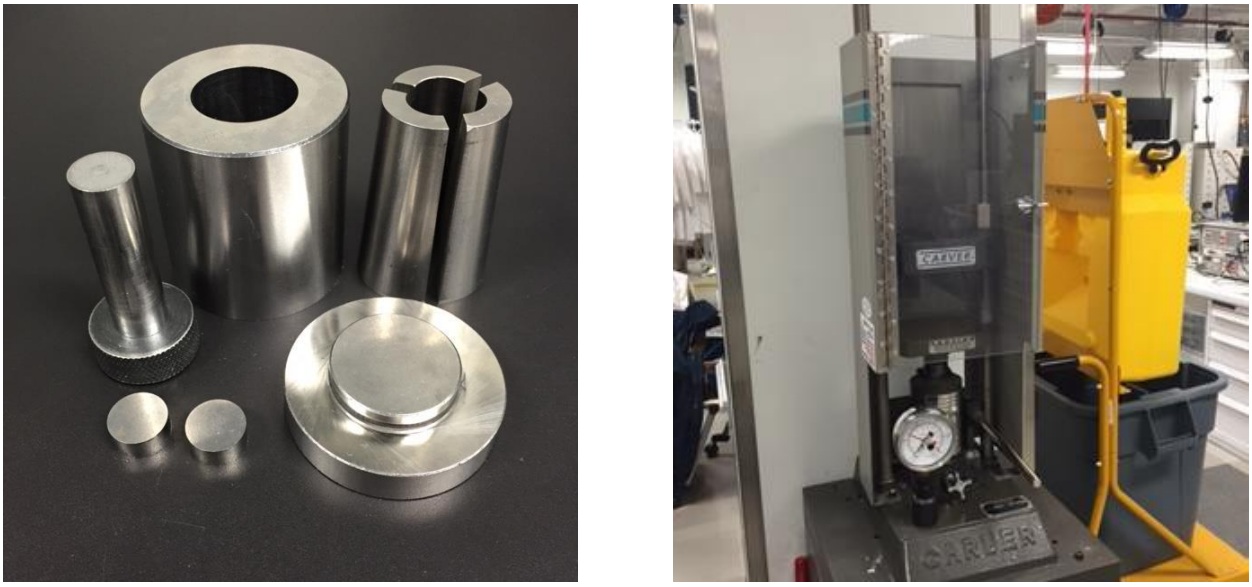

(a) (b)

Figure 3.1.3: Pressing equipment: (a) die set and (b) hydraulic press.

SHS was conducted in a hot-wire ignition setup (Fig 3.1.4). Samples were ignited inside the steel chamber in an argon environment. For the ignition of the mixture, a 1-g booster pellet of stoichiometric Ti/B mixture was placed at the top of the sample and ignited by a tungsten wire heated by a DC power supply.

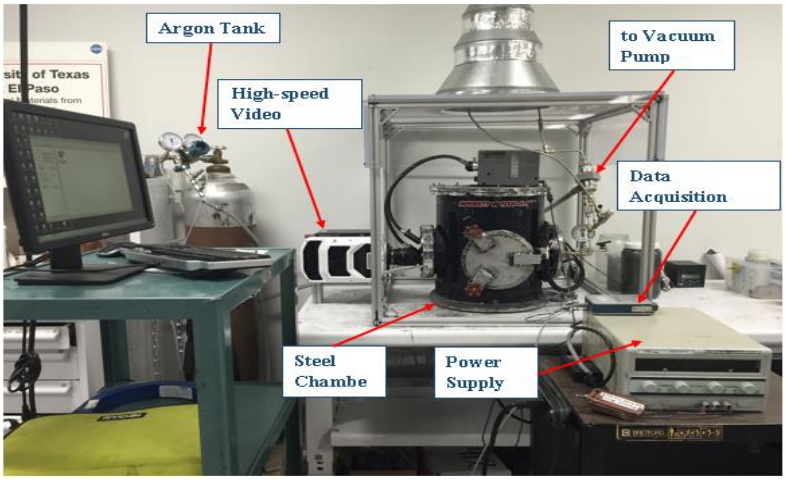

Figure 3.1.4: Hot-wire ignition setup.

Following SHS, products were leached in diluted hydrochloric acid (HCl) to remove MgO and NaCl. After leaching, powder composition was zirconium diboride with oxide impurities, which was determined by X-ray diffraction analysis.

3.1.2 Mixing

In the literature on sintering, volume fractions are usually used to characterize the compositions. For preparation of the mixtures, mass fractions were calculated using the following formula:

$$mf_{additive} = \frac{y_{additive}(\rho_{additive})}{y_{additive}(\rho_{additive}) + y_{ZrB_2}(\rho_{ZrB_2})}$$

Table 3.1.1 show the tested volume fractions and corresponding mass fractions. Interestingly, in the case of $MoSi_2$, the volume fraction and the mass fraction are close to each other because the densities of ZrB_2 (6.08 g/cm^3) and $MoSi_2$ (6.26 g/cm^3) are comparable.

Table 3.1.1: Volume and mass fractions for mixtures.

Additive	**Density (g/cm^3)**	**Volume fraction of ZrB_2**	**Volume fraction of additive**	**Mass fraction of ZrB_2**	**Mass fraction of additive**
B_4C	2.52	0.8	0.2	0.906	0.094
$MoSi_2$	6.26	0.9	0.1	0.897	0.103

Before mixing, the ZrB_2 powder was ground using an agate pestle and mortar for 5 min. The powders of ZrB_2 and the additive were weighed using a scale (Mettler Toledo, ML303E), placed in zirconia-coated bowls, and mixed in a 3D inversion kinematics tumbler mixer (Inversina 2L, Bioengineering, Fig. 3.1.1) for 40 min.

3.1.3 Milling

For the investigation of the milling effect in sintering, powders were milled using the planetary ball mill (see Section 3.1.1). Powders were placed in zirconia-coated grinding bowls (volume: 80 mL) with zirconia milling balls (diameter: 3 mm). The balls-to-powders mass ratio was 20:3. To prevent oxidation during milling, grinding bowls were filled with argon gas. Mixtures were milled for 1 and 5 min at 1000 rpm by cycles. Each milling cycle was composed of 1 min of milling followed by a cooling time of 60 min.

3.1.4 Compacting of Pellets

The final step for pellet preparation was compacting. Powders were placed inside a trapezoidal die set and compacted using a uniaxial hydraulic press (see Section 3.1.1). For larger diameters, larger pressing forces were used for pellet compaction.

As experiments progressed, pressing forces were increased with the objective of increasing the sample density prior to heating because it was hypothesized that increasing the initial density of the compact would lead to higher densities after heating. It should be noted that the manufacturer of the dies has limited pressing force to 3 metric tons for 6-mm diameter and to 10 metric tons for 13-mm diameter. Following this constraint, for 6-mm pellets the force was 3 metric tons (pressure: 1040 MPa) and for 13-mm pellets the force was 10 metric tons (pressure: 738 MPa).

3.2 Sintering Experiments

Sintering was conducted in a 30kW 2000 °C induction heating system (MTI Corporation, EQ-SP-50KTC, Fig. 3.2.1) in an argon environment at an absolute pressure of about 1 torr. Argon was flowing continuously through the furnace at a flow rate of about 200 mL/min. The pressure was measured using a pressure transducer (Infinicon, PCG554) and the flow rate was measured using a rotameter. The reduced pressure argon environment was created using a vacuum pump (MTI Corp., VRD-8) while constantly feeding argon into the system. Samples were placed in a graphite crucible (dimensions: 2" OD x 1.4" ID x 3.75" Deep). The crucible was placed inside a three-layer refractory liner, which was located inside a quartz tube (see Fig.3.2.1). The gas temperature in the furnace (inside the crucible, about 0.5” below the top) was measured by a W5%Re/W26%Re (C-type) thermocouple. Using a programmed controller, the

temperature was increased linearly with a heating rate of 10 °C/min. After a 60-min plateau at the maximum temperature, the furnace was turned off and the sample was cooled naturally.

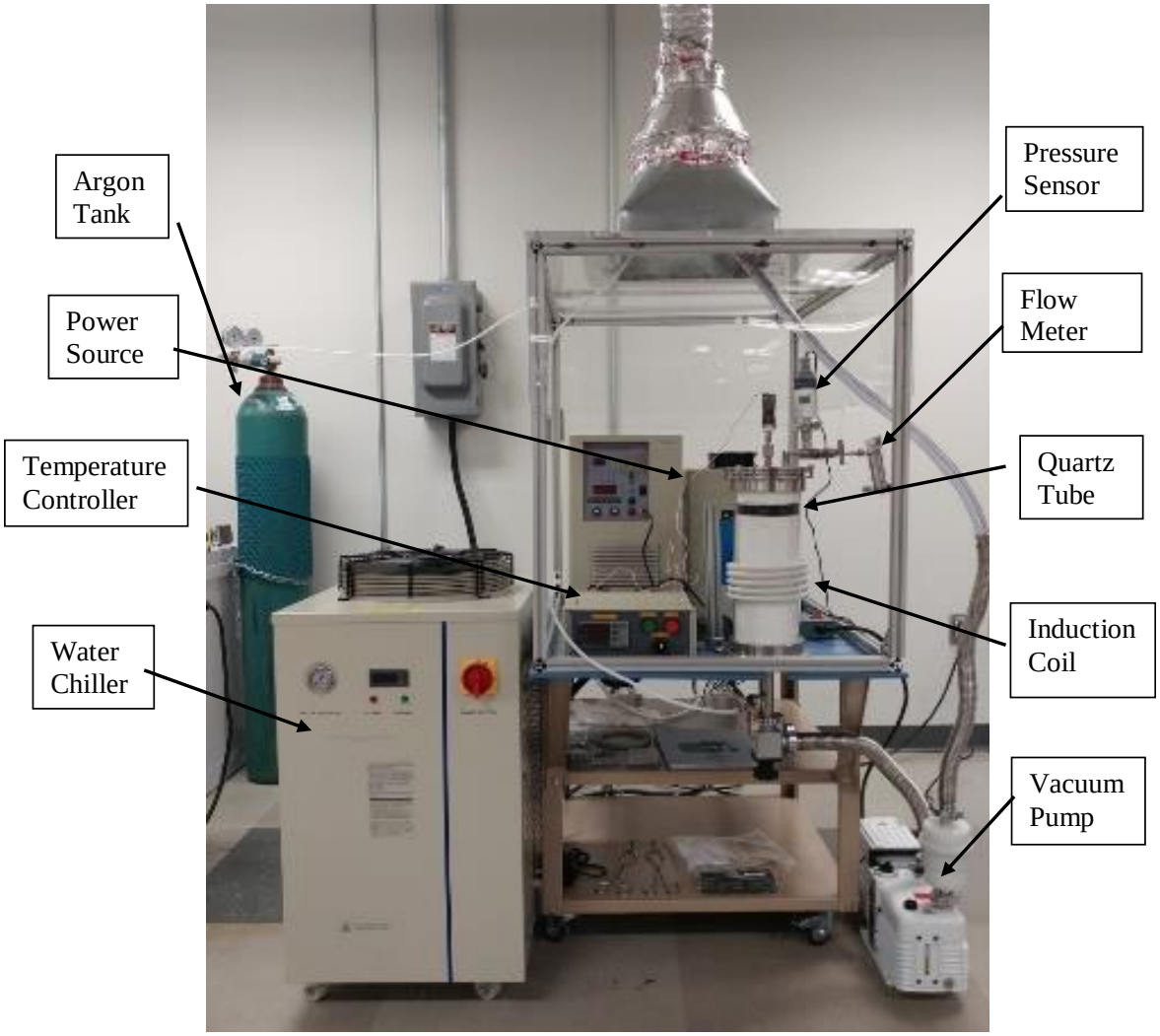

Figure 3.2.1: Induction heating system

Sintering experiments were conducted with the products obtained by MASHS of $ZrO_2/B_2O_3/Mg/NaCl$ mixtures with 20% excess Mg and 10 – 30 wt% NaCl. After combustion, MgO and NaCl were removed by leaching in a diluted HCl. This resulted in a powder that consisted mainly of zirconium diboride and relatively small amounts of zirconia and boron

oxide. Different heating profiles were tested in order to find the most effective one. Sintering experiments had two objectives: the consolidation of the compact sample and the removal of oxides.

The first profile consisted of a single ramp of 10 °C/min, starting at 25 °C and ending at 1800 °C, followed by a 1-h isothermal step at 1800 °C. The second profile was composed of two isothermal steps, at 1500 °C for 30 – 60 min, and at 1850 °C for 1 h. Heating rates for ramps stayed consistent throughout all experiments.

To improve experimental parameters, different setup configurations were tested. During initial experiments, samples were placed far away from the thermocouple tip, which could have potentially resulted in a significant difference between the gas temperature measured by the thermocouple and the actual temperature of the sample. Another adverse effect of initial setups was that the sample was in direct contact with the graphite crucible, which could have promoted the formation of zirconium carbide for some samples. Several attempts at mitigating these adverse effects were made. One method was moving the sample closer to the thermocouple tip and isolating the sample from the graphite crucible by filling the crucible with zirconia powder up to one inch away from the top and placing samples inside an alumina crucible separated by thin alumina disks. The induction coil was moved accordingly. The induction coil is fixed to the power source, in order to raise the coil a stand was made to lift the power source. Figure 3.2.2 shows the setup before and after this modification.

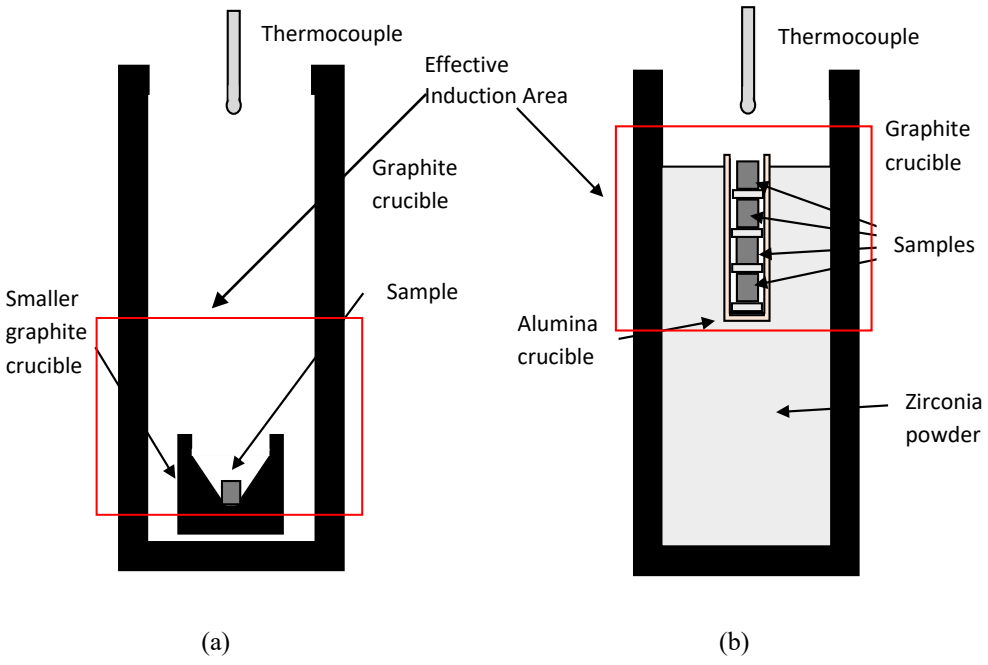

Figure 3.2.2: Schematic diagrams of (a) initial setup and (b) modified setup.

Unfortunately, though this did bring the samples closer to the thermocouple, the samples collapsed, and it became impossible to distinguish from one another. This led to a second modification. This consisted of stacking smaller graphite crucibles on top of each other and separating the top crucible with a disk made from compacted zirconia powder, and separating samples by the same method. This method proved successful; it brought samples closer to the thermocouple tip and samples were isolated from the graphite crucible and each other. Figure 3.2.3 shows the final setup.

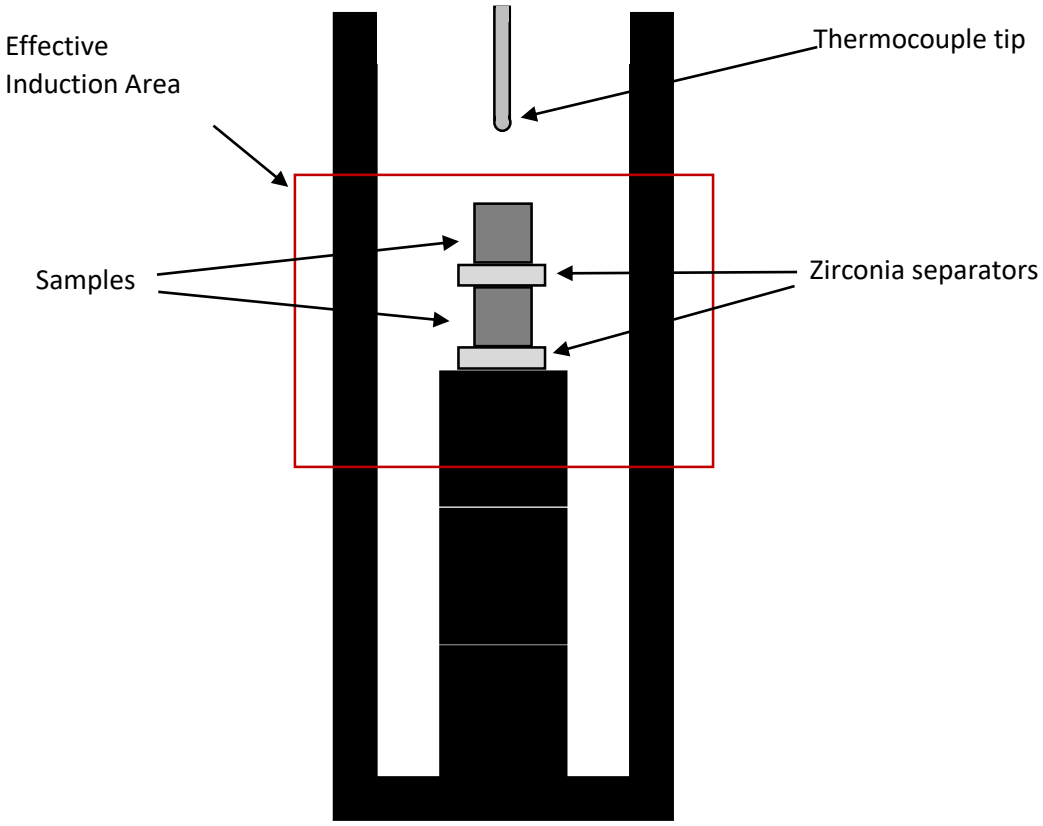

Figure 3.2.3: Schematic diagram of the final setup.

During experiments, unrelated to the modifications made inside the graphite crucible, problems occurred with the setup. The three-layer refractory liner and the thermocouple tip experienced damage (see Fig. 3.2.4).

(a) (b)

Figure 3.2.4: Pictures of (a) a hotspot on the surface of the induction furnace and (b) a damaged thermocouple tip.

Unfortunately, there is no easy remedy for the three-layer refractory liner, which required frequent replacement. However, there were two remedies put in place for prolonging the lifespan of the thermocouple. The first was to remove oxide impurities from argon using heated titanium sponge inside a tube furnace operating at 800 °C (see Fig. 3.2.5). The second was to coat the tip of the thermocouple with tungsten.

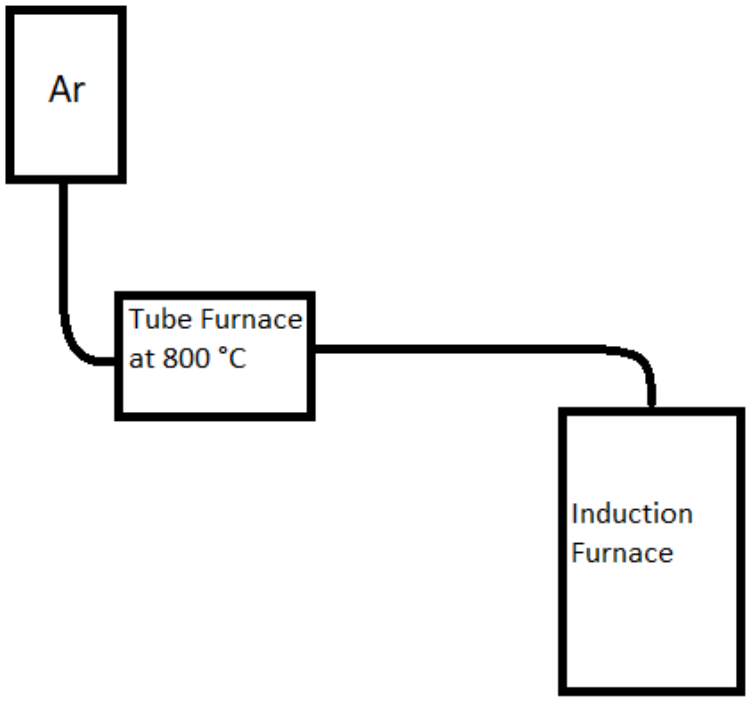

Figure 3.2.5: Schematic of Ar feeding system

3.3 Material Characterization

3.3.1 Density Measurements

The mass of the pellet was measured using a scale (Mettler Toledo, ML303E). The dimensions of the pellets were measured using a digital caliper. Relative density was calculated by dividing the measured density by the theoretical density. For these calculations, it was assumed that the composition was purely zirconium diboride.

3.3.2 X-Ray Diffraction Analysis

Composition of samples before and after sintering were studied using X-ray diffraction analysis (Bruker D8 Discover XRD, Cu k-alpha 1, 0.154 nm, Fig. 3.2.2). Scan speed was 1°/min with a step size of 0.02°.

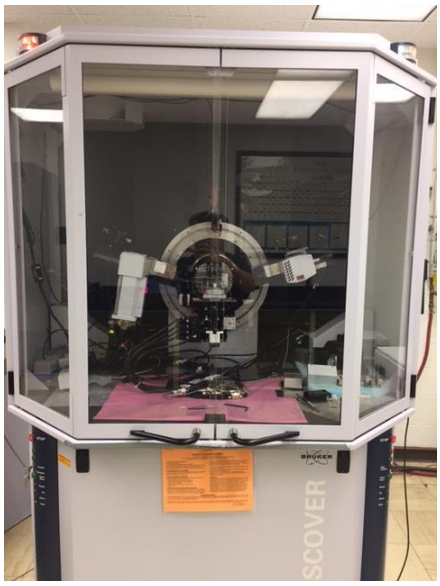

Figure 3.3.2: X-ray diffractometer (Bruker D8 Discover XRD, Cu k-alpha 1, 0.154 nm)

3.3.3 SEM Imaging

The morphology of heated samples was studied a scanning electron microscope (SEM, Hitachi S-4800) with a secondary electrons detector. Samples were ground down to a thickness of 1 mm using a grinding table.

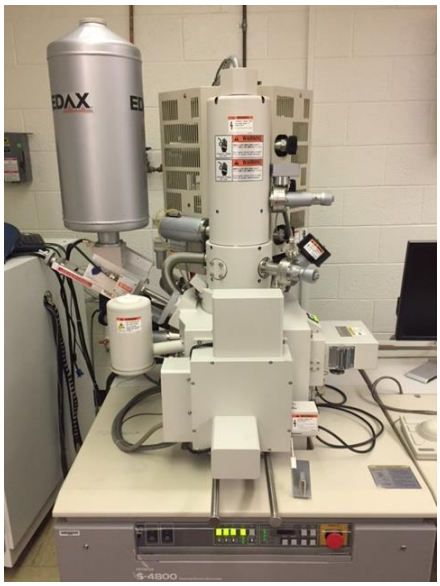

Figure 3.3.3: Scanning electron microscope (Hitachi S-4800).

3.3.4 Particle Size Analysis

Particle size distribution was determined for powders before and after milling with a laser diffraction particle size analyzer (Microtrac Bluewave). To avoid oxidation or dissolution, experiments were conducted using isopropyl alcohol as a sample carrier.

Figure 3.3.4: Particle size analyzer (Microtrac Bluewave).

Chapter 4: Results and Discussion

4.1 Sintering Experiments with no Additives

Initial experiments were conducted without additives to study the effect of heating on the powders obtained by mechanically activated self-propagating high-temperature synthesis (MASHS). The first goal of the sintering experiments was the densification of compacted powders obtained by MASHS. The second goal was to remove or reduce the oxide impurities, specifically zirconia and boron oxide. Note that, according to the literature, boron oxide can easily be removed by evaporation with a temperature step included in the heating profile. The challenge is removing the remaining zirconia.

Initial experimentation was conducted with unmilled samples using a maximum temperature of 1800 °C. Figure 4.1.1 shows the XRD pattern after heating. It seen that small peaks of zirconia still appear, which is undesirable for the application of the final product, which requires a high electrical conductivity, something that is reduced by the presence of zirconia. It is unknown whether boron oxide was removed because it is amorphous, so it would not appear in XRD patterns. The relative density after heating was approximately 38%, which is very low and undesirable.

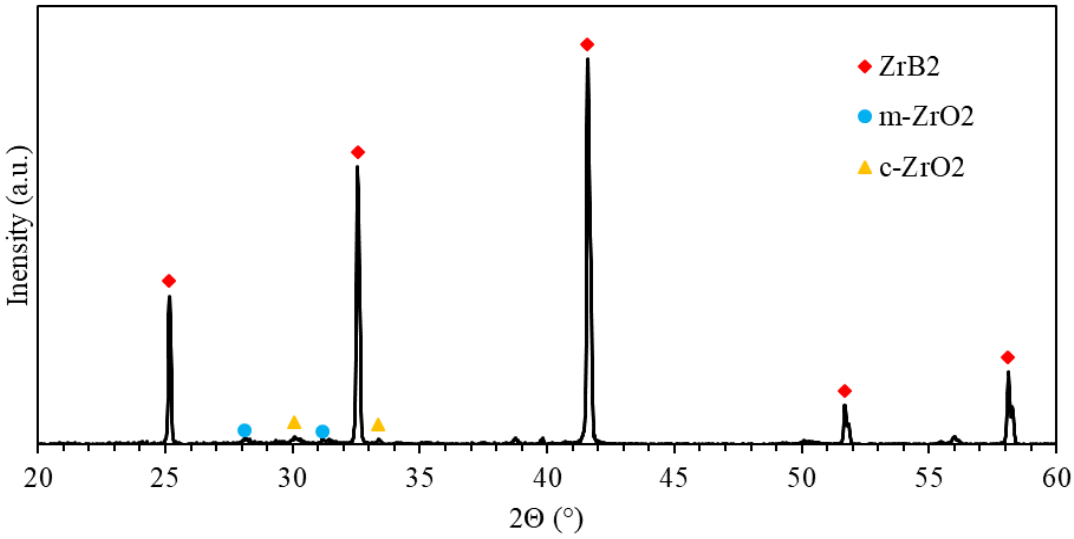

Figure 4.1.1: MASH ZrB_2 after heating at 1800 °C without additives.

The next step was to increase the maximum heating temperature to 2000 °C to explore the possibility of removing zirconia. This proved to be successful but had one major drawback: the equipment was damaged as a result of operation at 2000 °C, making it an undesirable experimental parameter. For this reason, different routes had to be explored in order to eliminate zirconia from samples. The XRD pattern is shown in Fig. 4.1.2, where one can see the sole presence of zirconium diboride, with no other peaks. This indicates that zirconia was completely removed. However, this was conducted with unmilled powders, which resulted in a low relative density of 38%.

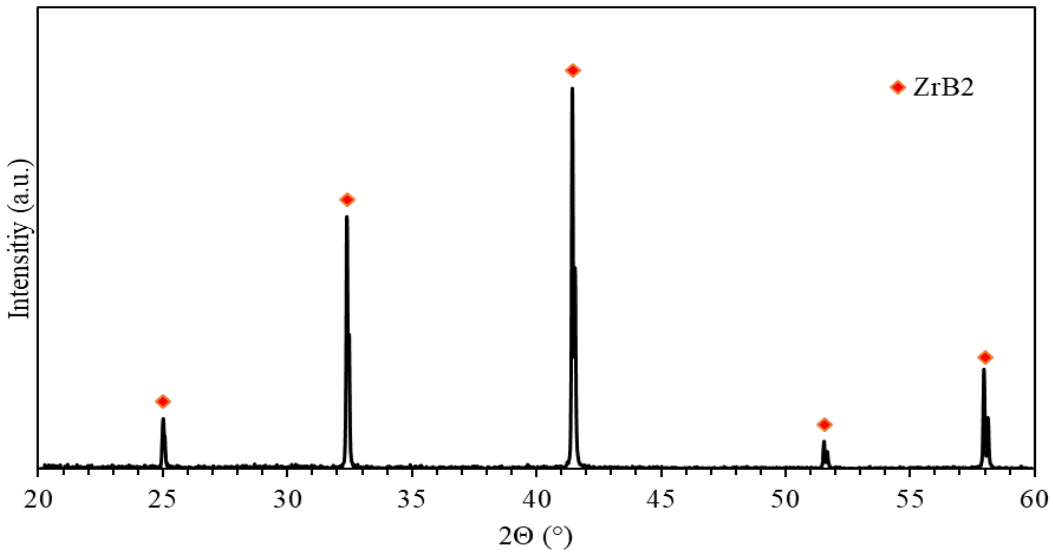

Figure 4.1.2: MASHS ZrB_2 after heating at 2000 °C with no additives.

4.2 Effect of Additives

Two additives were tested, molybdenum silicide and boron carbide. For molybdenum silicide there was apparently a full reduction though smaller peaks were difficult to identify (see Fig. 4.2.1). A positive result was that the temperature for eliminating zirconia dropped from 2000 °C to 1850 °C, which was better for the lifespan of the setup.

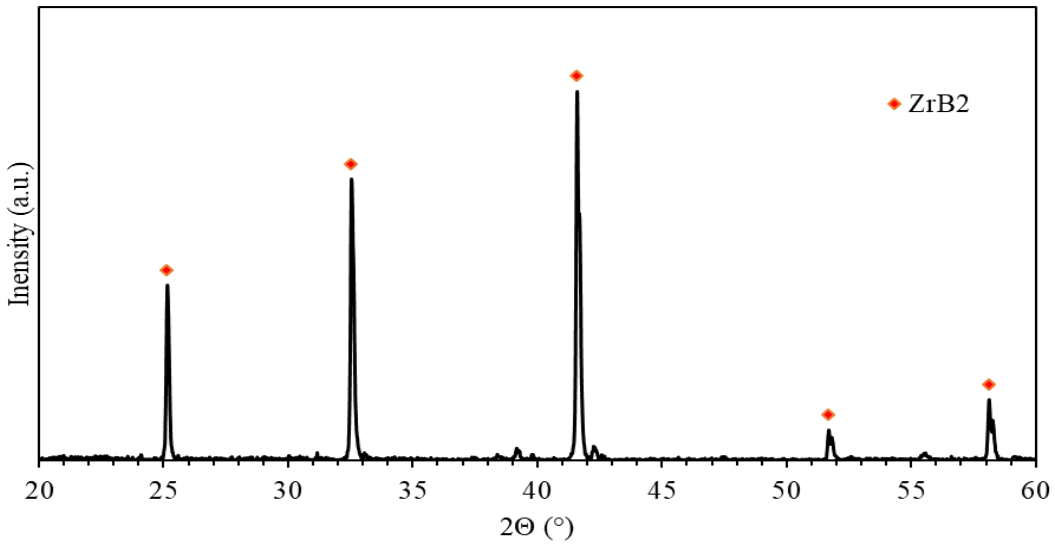

Figure 4.2.1: MASHS ZrB_2 after heating at 1850 °C with $MoSi_2$

Two heating profiles were used for experiments with 20 vol% boron carbide. In one of them, the temperature increased linearly up to 1850 °C. In the other one, the maximum temperature was the same, but the temperature increase was interrupted with a 30-min isothermal step at 1500 °C. This isothermal step was used for the vaporization of boron oxide. Figure 4.2.2 shows the XRD pattern of the sample in the experiment with no plateau. It is seen that the product is a single zirconium diboride phase with very small peaks of impurities, which were not identified. The relative density of the product was approximately 32%, lower than in the previous experiments.

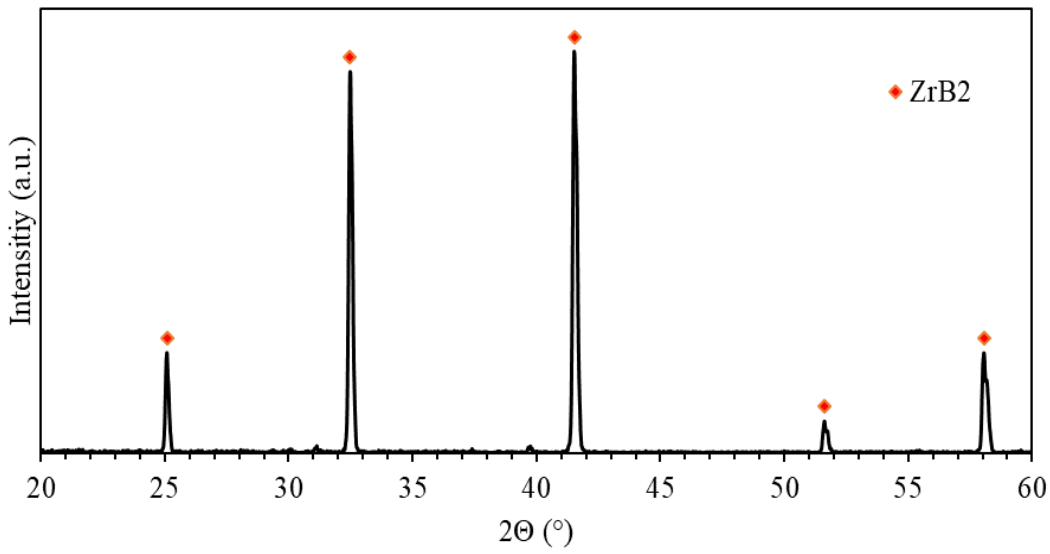

Figure 4.2.2: MASHS ZrB_2 after heating at 1850 °C with 20 vol% B_4C

The XRD pattern of the sample that was heated with the plateau at 1500 °C revealed strange results. Figure 4.2.3 shows the XRD pattern. The dominant phase is zirconium carbide, while the peaks of zirconium diboride being much smaller.

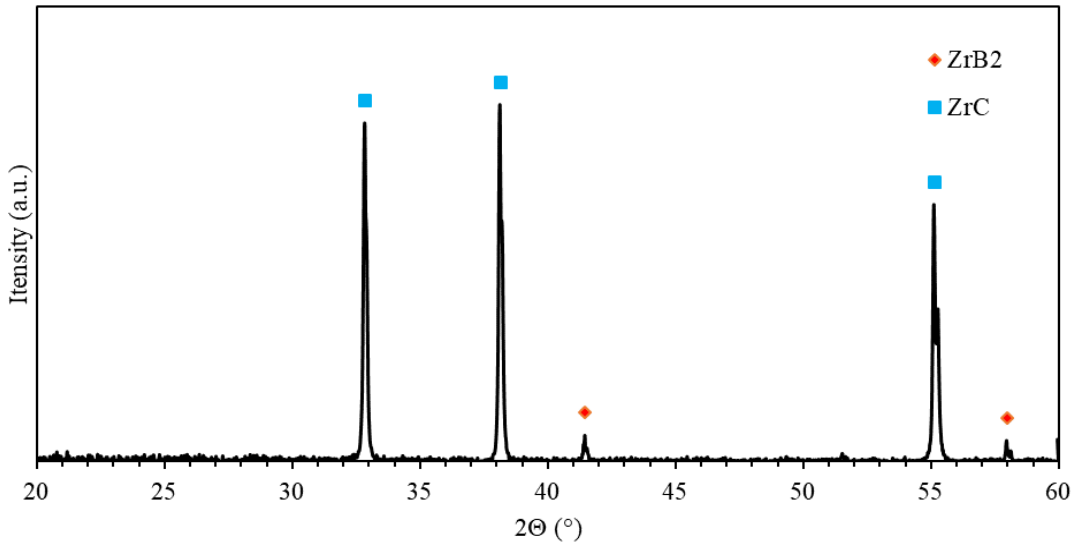

Figure 4.2.3: MASHS ZrB_2 with 20 vol% B_4C after heating at 1850 °C with a plateau at 1500 °C

For the first modification of the setup, which was shown in Fig. 3.2.1, four samples were tested. Two were made of zirconium boride obtained by MASHS, while the other two were made from commercial zirconium boride powder for comparison. One pellet from each powder group had 20 vol% boron carbide. All pellets were exposed to 1850°C as a maximum temperature.

Unfortunately, as mentioned in Chapter 3.2, the experiments conducted in the first modification of the setup resulted in the destruction of the alumina crucible during heating, which consequently resulted in the submerging of all samples in the zirconia powder. When retrieving the samples, it was impossible to identify them. Retrieved pellets were numbered from 1 to 4 in XRD patterns that are shown to illustrate the negative results obtained from using this setup.

Figure 4.2.4 shows the XRD pattern of sample #1. The taller peaks show the presence of zirconium carbide, while smaller peaks show zirconium oxide and zirconium diboride. The calculated relative density for this sample after heating was 44%. It is possible that based on the composition, the initial sample composition was commercial ZrB_2 with 20 vol% boron carbide. ZrC is typically not present in samples with an initial composition of commercially obtained zirconium diboride. It is possible that the sample was submerged in zirconia where it was oxidized, and later reacted with boron carbide to form ZrC during collapse of the setup shown in Fig. 3.2.2.

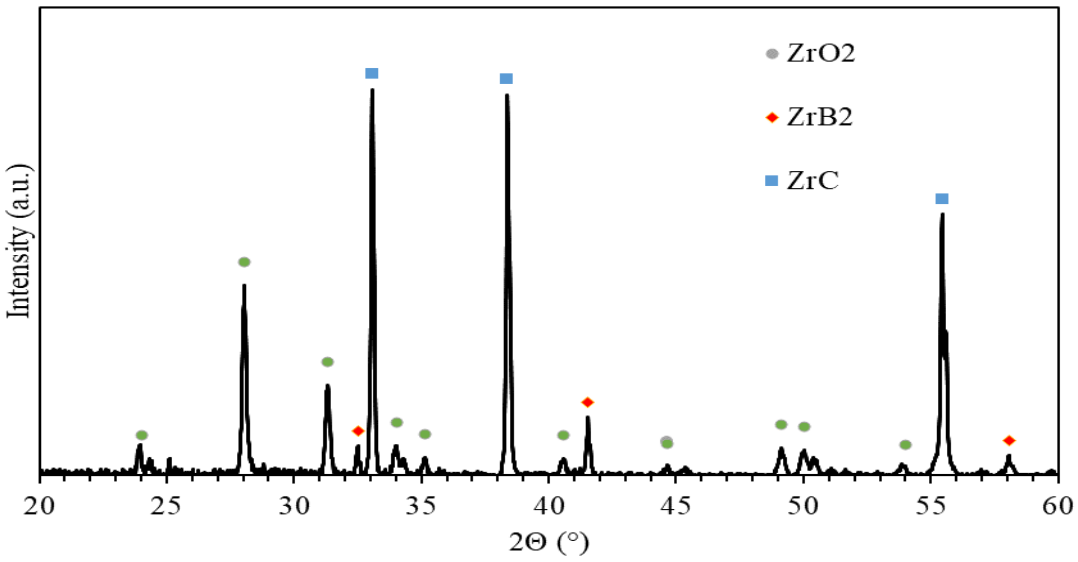

Figure 4.2.4: XRD pattern of sample #1

Figure 4.2.5 shows the XRD pattern of sample #2. Only peaks of zirconium carbide and zirconium oxide are present. The calculated relative density of this sample after heating was about 49%. Experiments after these results do not show formation of zirconium carbide when using commercial powder. It can be hypothesized that ZrC formed because of oxides that are present in zirconium diboride obtained by MASHS. This leads to the posibility that the initial composition of this sample was MASHS zirconium diboride with no additives. It is possible that the sample was contaminated through contact with other samples which had boron carbide additions, which could explain the relatively smaller peaks compared to taller zirconia peaks.

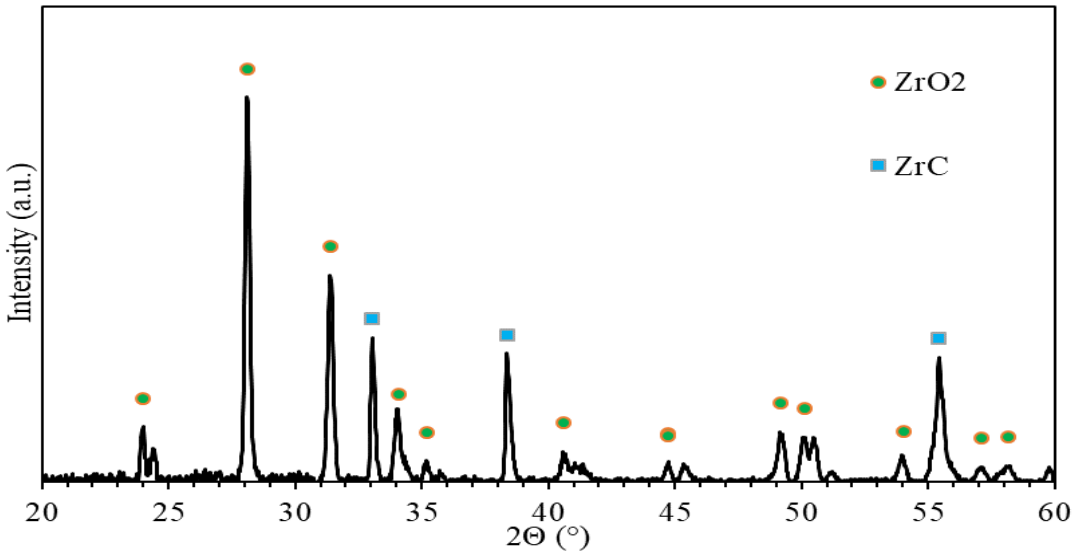

Figure 4.2.5: XRD pattern of sample #2

Figure 4.2.6 shows the XRD pattern of sample #3. There are only peaks of zirconium oxide. The calculated relative density for this sample was 74%. From examining the sample, it appears that the alumina disk melted onto one of the sides, which could explain a higher density calculation in comparison to the others. It is very possible that the initial composition of this sample was commercial zirconium diboride and it was oxidized during submersion in the zirconia powder.

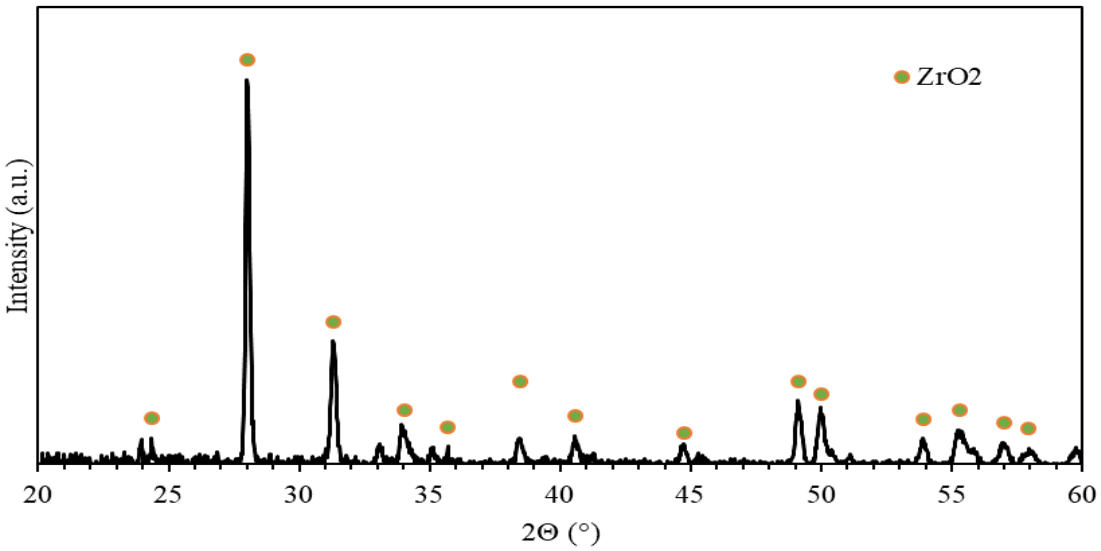

Figure 4.2.6: XRD pattern of sample #3

Figure 4.2.7 shows the XRD pattern of sample #4. Tall peaks of both zirconium carbide and zirconium oxide are observed. The calculated relative density for this sample after heating was 43%. Finally, from comparing tall peaks of zirconium carbide to relatively smaller peaks of zirconia, it is most likely that the initial sample composition was mash zirconium diboride with 20 vol% B_4C.

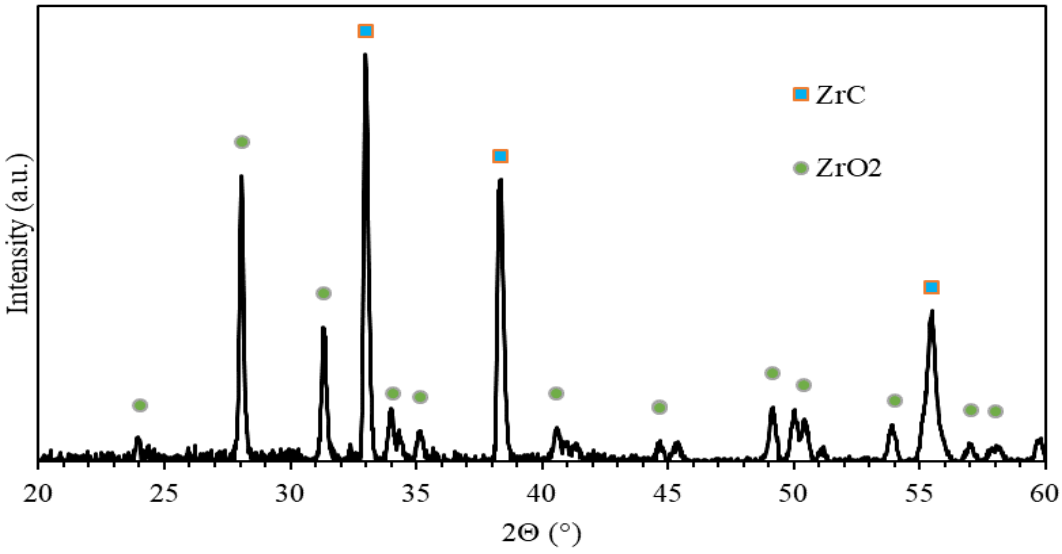

Figure 4.2.7: XRD pattern of sample #4

Three sample compositions were tested using the updated argon feeding system. Two were made of zirconium diboride obtained by MASHS (one with 20 vol% B_4C and one without B_4C), while the third was made from commercial zirconium diboride (99.5% metal basis excluding Hf, -325 mesh, Alfa Aesar) with 20 vol% boron carbide.

Figure 4.2.8 shows the XRD pattern of the sample made of commercial zirconium diboride with 20 vol% boron carbide after heating. All major peaks are zirconium diboride. Initial sample density was 57% and density after heating was 48%.

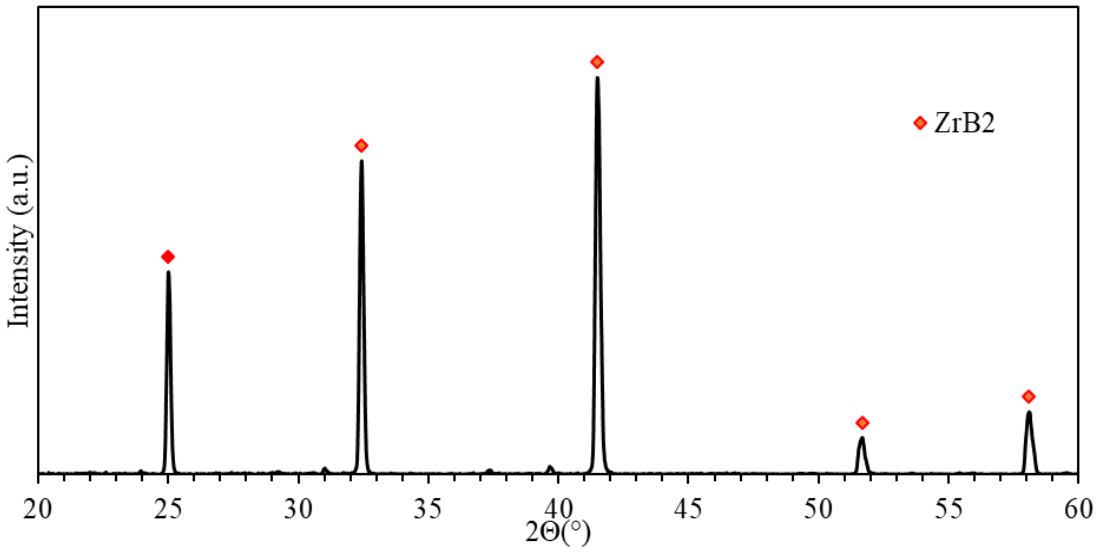

Figure 4.2.8: Commercial ZrB_2 with 20 vol% B_4C after heating at 1850 °C with a 30-min intermediate plateau at 1500 °C

The sample of MASHS zirconium diboride with 20 vol% boron carbide was exposed to the same heating profile as the sample of commercial zirconium diboride with 20 vol% boron carbide. The sample with MASH zirconium diboride had lower densities in comparison. The initial density (after pressing) was 50% and it dropped to 42% after heating. The XRD pattern for this sample after heating is shown in figure 4.2.9. Major peaks are zirconium carbide with small peaks of zirconium diboride.

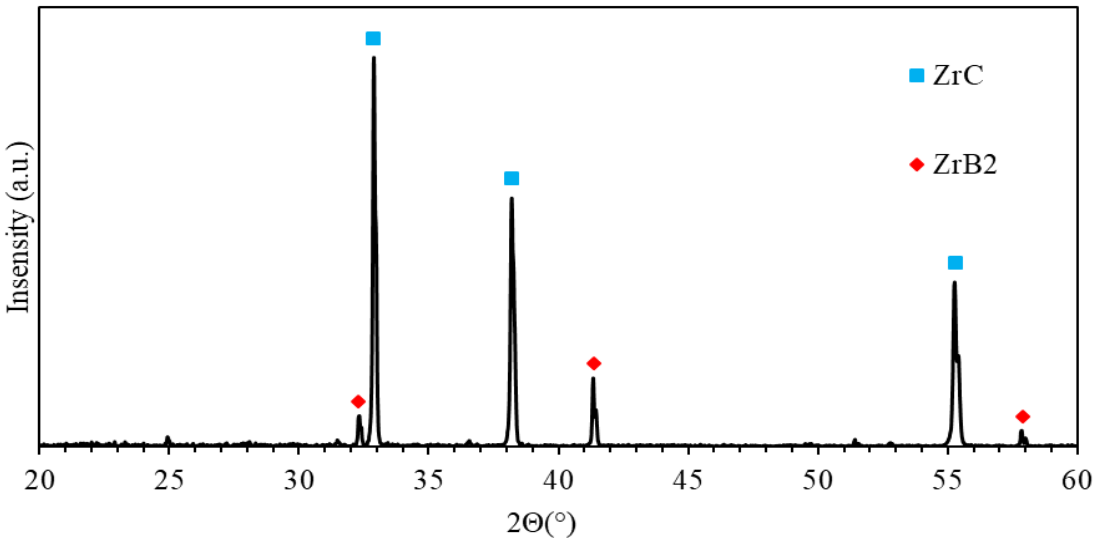

Figure 4.2.9: MASH ZrB_2 with 20 vol% B_4C after heating at 1850 °C with a 30-min intermediate plateau at 1500 °C

The third sample, composed of only MASH zirconium diboride, was exposed to a different heating profile than the other two. It had a single steady ramp of 10°C/min up to 1850°C with a holding time of 1 h. Initial density of the sample was about 53% and it dropped to about 36% after heating. The XRD pattern shown in figure 4.2.10 shows major peaks of zirconium diboride.

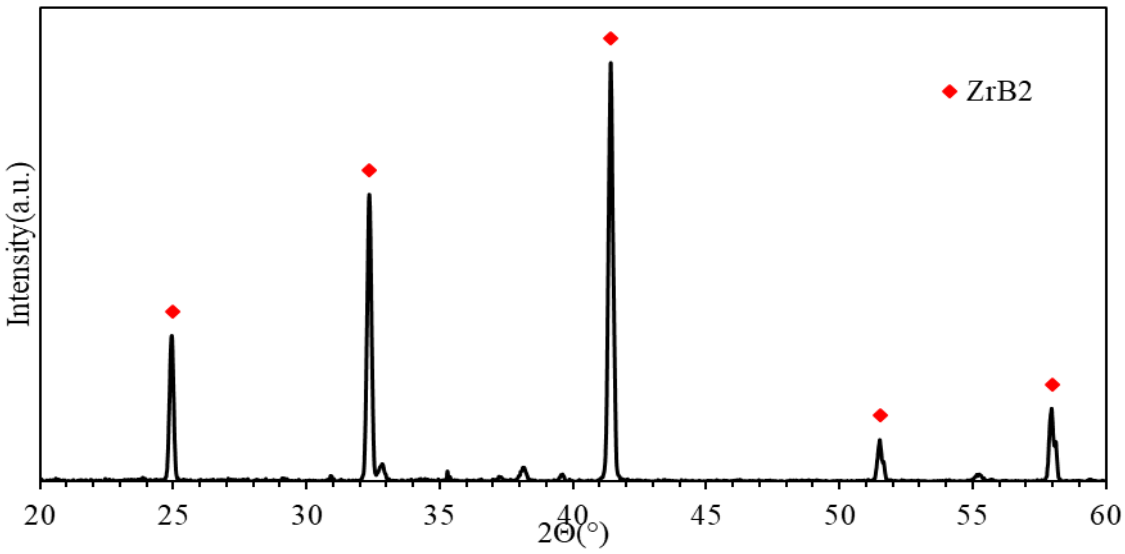

Figure 4.2.10: MASH ZrB_2 with no additives after heating at 1850 °C with a 30-min intermediate plateau at 1500 °C

XRD patterns for samples of commercial ZrB_2 with 20 vol% B_4C and of MASHS ZrB_2 with 20 vol% B_4C have one major difference. The presence of ZrC is only observed for samples with ZrB_2 from MASHS. A possible hypothesis is that there is little to no surface oxide in the form of ZrO_2 for the C in B_4C to react with for samples with commercial ZrB_2. The presence of boron oxide is still possible for commercial zirconium diboride, but this is eliminated through evaporation.

4.3 Effect of Milling

The experiments with non-milled powders have shown that they reached relative densities no higher than 55% as a result of pressing. After heating, the relative density of samples dropped to as low as 32%. This led to efforts in analyzing the effect of milling on density.

Due to long processing times for MASHS powders, the effect of milling was first analyzed using commercial ZrB_2. Two sample compositions were tested. The first composition

was only ZrB_2 and the second composition was ZrB_2 with 20 vol% B_4C. Two milling times were explored, 1 min and 5 min. Both mixtures reached a relative density of about 60% and 70% respectively. After heating, for samples with no additives, densities remained constant, while for samples with 20 vol% B_4C density slightly increased. Relative density increased to approximately 65% for 1 min milling and to about 75% for 5 min milling. These results are understandable because milling results in a smaller particle size and reduces the surface energy, while B_4C eliminates surface oxides that inhibit densification through grain growth. The combination of milling and B_4C is required for promoting densification.

Figure 4.3.1 shows the XRD pattern of commercial zirconium diboride with no additives after heating with a milling time of 1 min. Since no additives were used, all peaks correspond to ZrB_2.

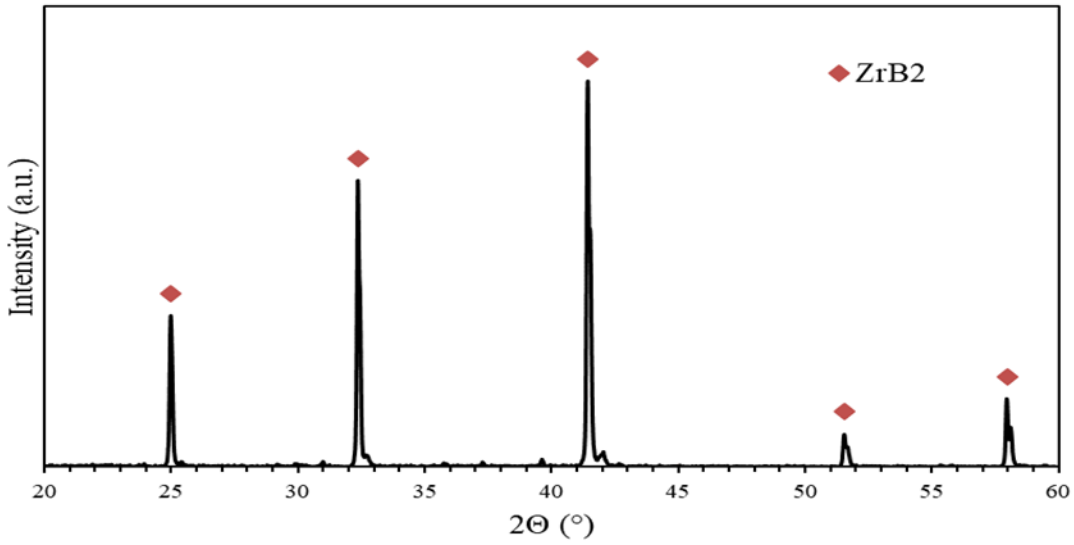

Figure 4.3.1: Commercial ZrB_2 with no additives after heating at 1850 °C with an intermediate plateau at 1500 °C (1 min milling).

Figure 4.3.2 shows the XRD pattern of commercial zirconium diboride with no additives with a milling time of 5 min. As for the previous sample, since no additives were used for heating, all peaks belong to ZrB_2.

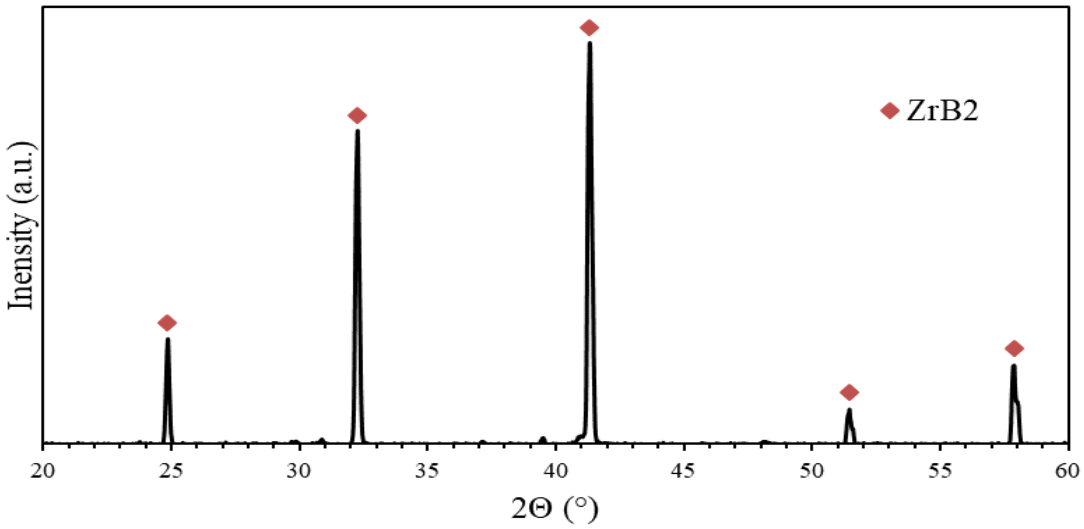

Figure 4.3.2: Commercial ZrB_2 with no additives after heating at 1850 °C with an intermediate plateau at 1500 °C (5 min milling).

Figure 4.3.3 shows the XRD pattern of commercial zirconium diboride with 20 vol% boron carbide with a milling time of 1 min after heating. All peaks correspond to ZrB_2. As mentioned in the previous section, the absence of ZrC peaks could be explained because there are no surface oxides in the form of ZrO_2 for B_4C to react with, therefore ZrC is not formed.

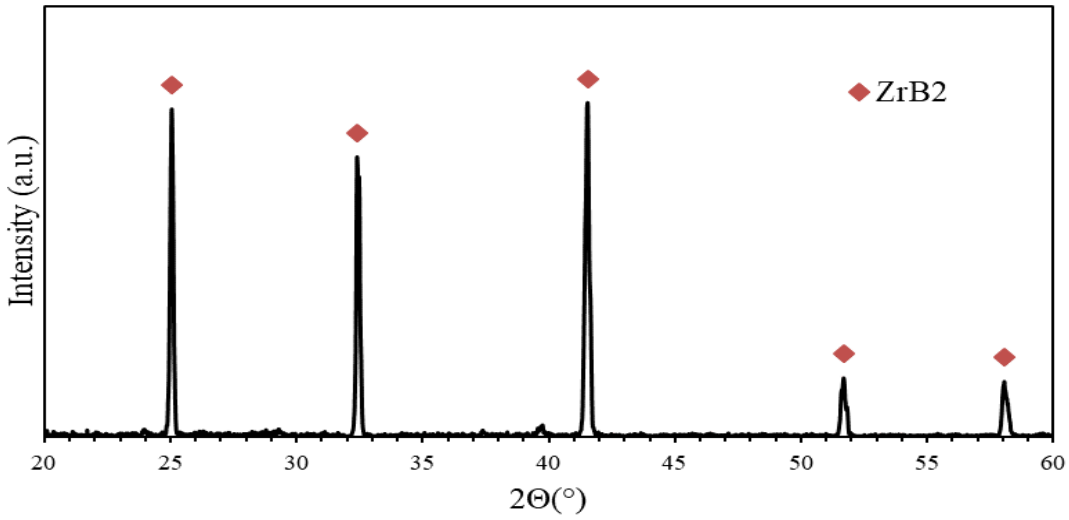

Figure 4.3.3: Commercial ZrB_2 with 20 vol% B_4C after heating at 1850 °C with an intermediate plateau at 1500 °C (1 min milling).

Figure 4.3.4 shows the XRD pattern of commercial zirconium diboride with 20 vol% boron carbide with a milling time of 5 min. Again, all peaks correspond to ZrB_2.

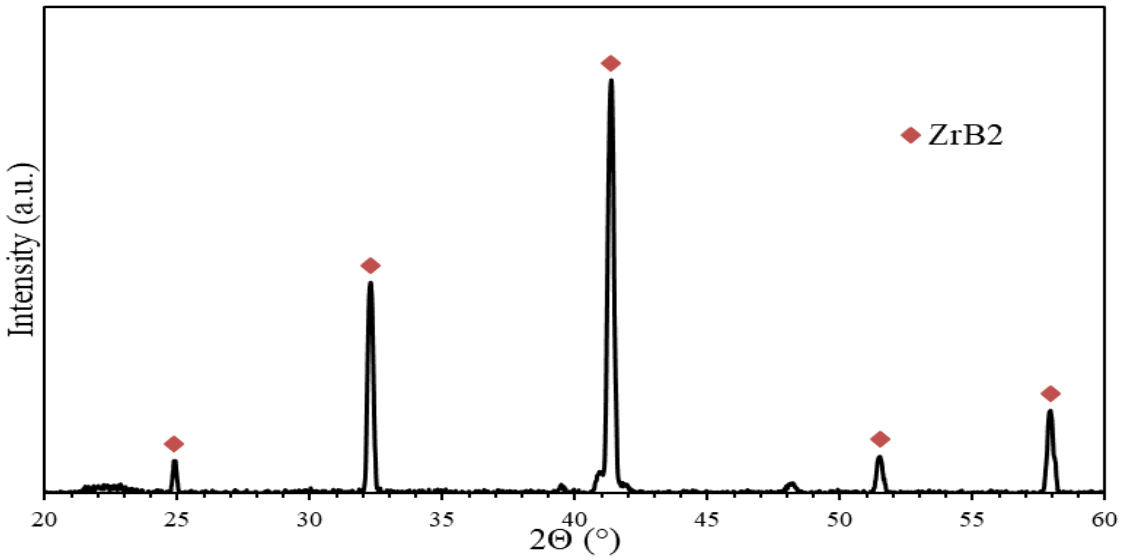

Figure 4.3.4: Commercial ZrB_2 with 20 vol% B_4C after heating at 1850 °C with an intermediate plateau at 1500 °C (5 min milling).

Figure 4.3.5 shows SEM images of ZrB_2 samples milled for 1 min, pressed, and heated without any additive (left) and with boron carbide (right). Areas where voids (black spots) are seen are pores. The images clearly show that samples heated with boron carbide are less porous than samples heated without it.

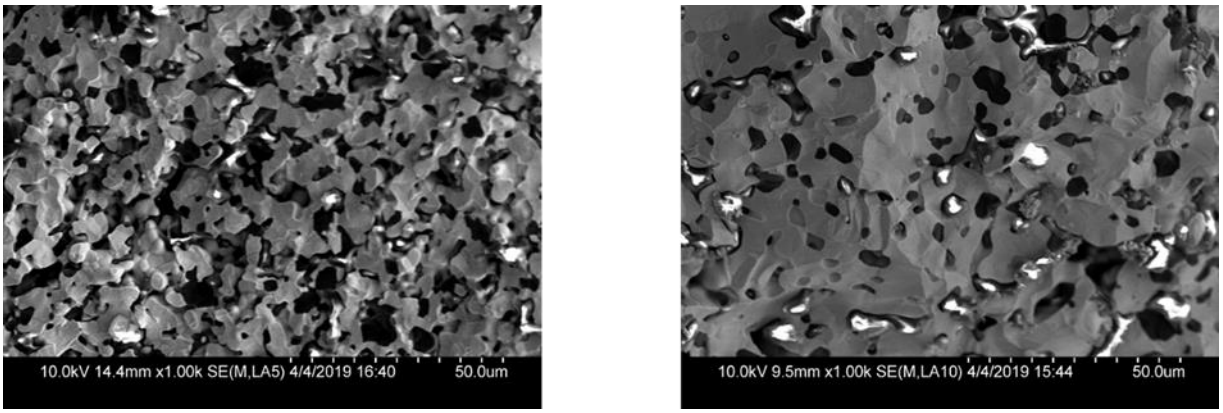

Figure 4.3.5: SEM image comparing the effect of additives on the porosity of samples: no additive (left) and 20 vol% boron carbide (right).

To better understand the effect of milling, the particle size distributions in powders before and after milling were studied for two compositions: (1) commercial ZrB_2 with 20 vol% B_4C and (2) MASHS ZrB_2 with 20 vol% B_4C. For each composition, the particle size distribution was determined for unmilled powders and for powders milled for 5 min. The measurements were conducted using the refractive index for zirconium (2.77), boron (2.34) and carbon (3.15). Using each refractive index, the particle size parameters were determined for irregular shaped particles and spherical particles. The table below shows results for each powder composition (smallest mean volume diameter to largest mean volume diameter)

Table 4.3: Mean volume diameters for sample compositions and milling times.

Composition	Mean Volume Diameter (μm)
Commercial ZrB_2 with 20 vol% B_4C unmilled	1.785 - 2.615
Commercial ZrB_2 with 20 vol% B_4C milled for 5 min	0.518 - 0.793
MASHS ZrB_2 with 20 vol% B_4C unmilled	1.077 - 2.182
MASHS ZrB_2 with 20 vol% B_4C milled for 5 min	0.695 – 1.272

Figure 4.3.6 shows the particle size distribution with the smallest mean volume diameter for unmilled commercial ZrB_2 with 20 vol% B_4C. The particle size distribution is wide, ranging from 1 μm to 100 μm. This wide distribution is undesirable for sintering.

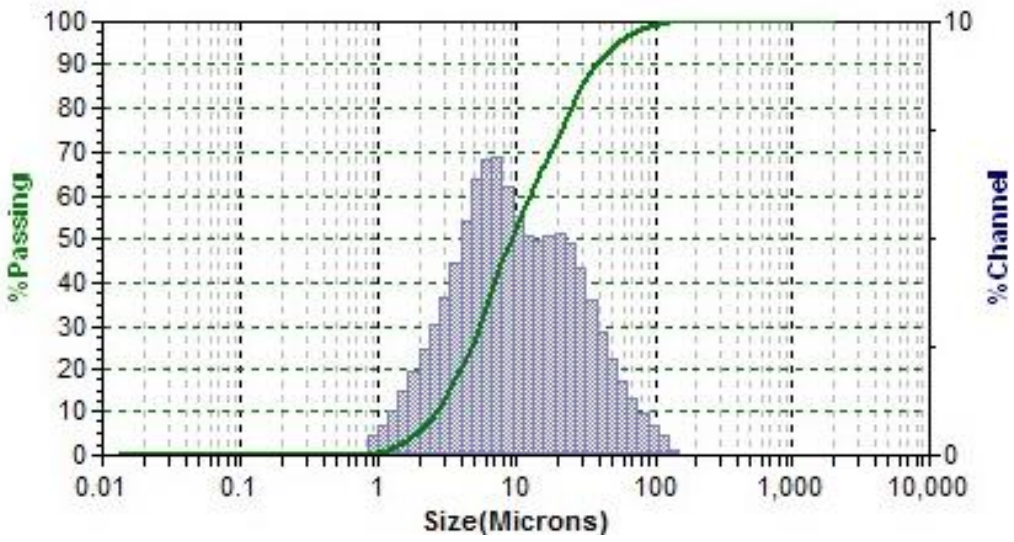

Figure 4.3.6: Particle size distribution for commercial ZrB_2 with 20 vol% B_4C.

Figure 4.3.7 shows the particle size distribution with the smallest mean volume diameter for ZrB_2 with 20 vol% B_4C milled for 5 min. Comparing it to the particle size distribution for unmilled powders, one can make two observations: (1) the distribution shifted toward smaller

particle sizes and (2) the distribution is more narrow. These smaller particle sizes may explain the high relative density of heated milled samples compared to heated unmilled powders.

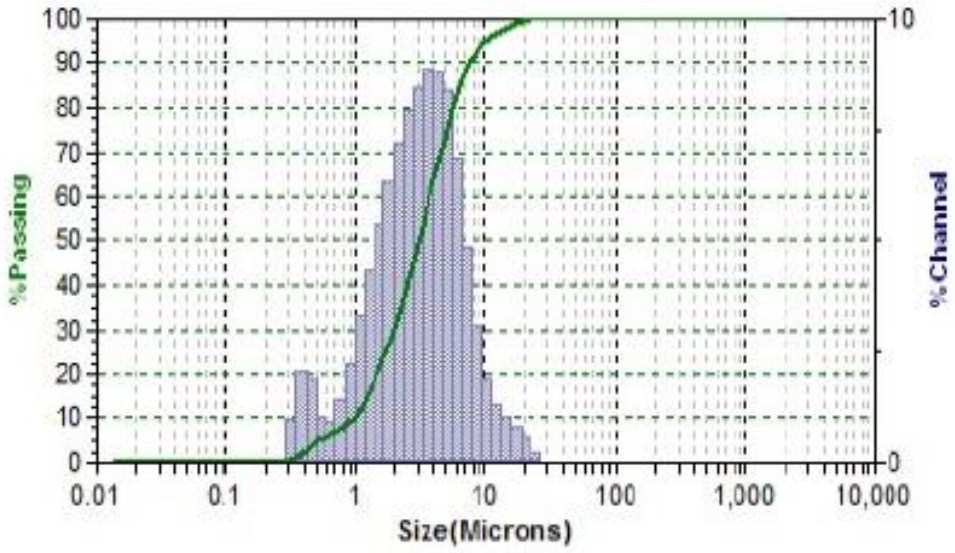

Figure 4.3.7: Particle size distribution for commercial ZrB_2 with 20 vol% B_4C with a milling time of 5 min.

Figure 4.3.8 shows the particle size distribution with the smallest mean volume diameter for unmilled MASHS ZrB_2 witih 20 vol% B_4C. The distribution is bimodal, with peaks at around 10 µm and 100 µm. The large number of coarse particles negatively affects sintering.

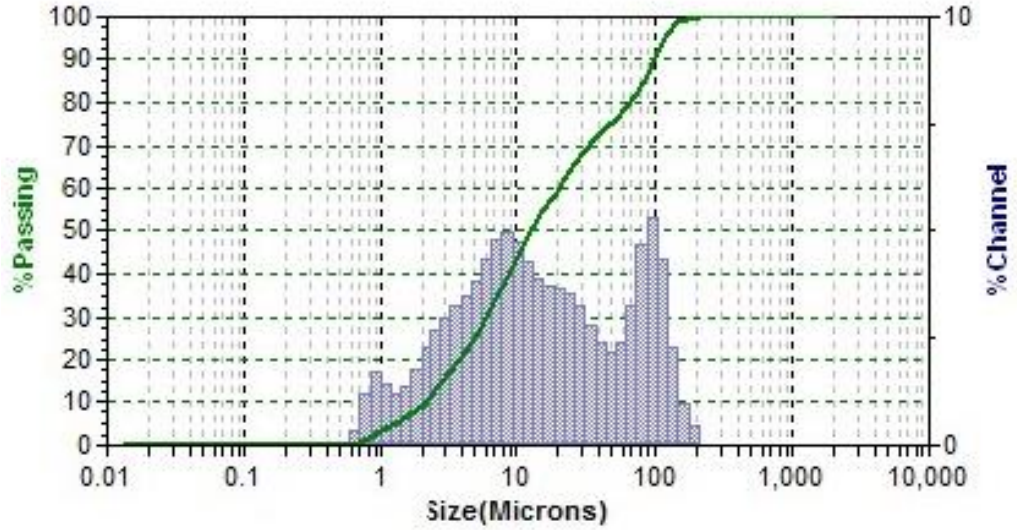

Figure 4.3.8: Particle size distribution for unmilled MASHS ZrB_2 with 20 vol% B_4C.

Figure 4.3.9 shows the particle size distribution with the smallest mean volume diameter for the same mixture after milling for 5 min. In contrast with the unmilled mixture, the distribution has a single peak at around 10 µm and it is clear that many coarse particles were milled to a much smaller size. This explains why milling is favorable for sintering.

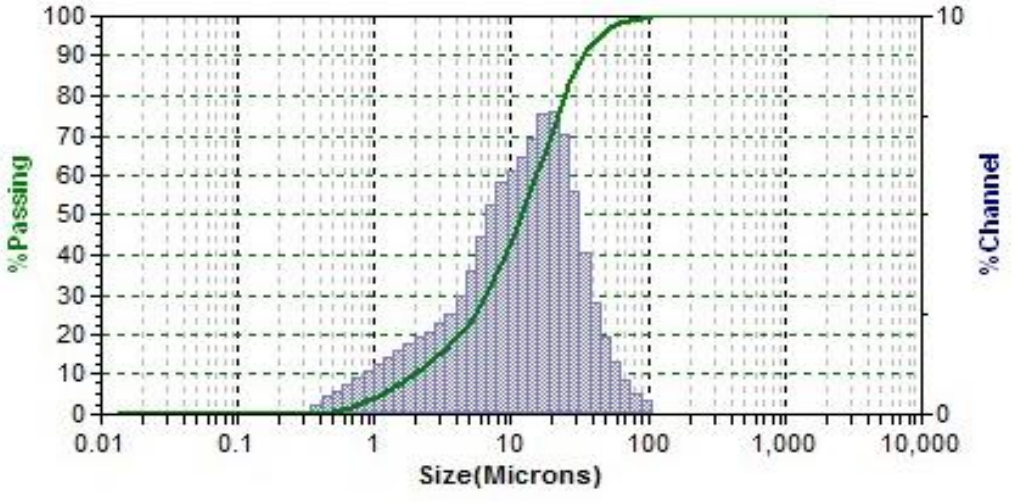

Figure 4.3.9: Particle size distribution for MASHS ZrB_2 with 20 vol% B_4C with a milling time of 5 min.

Chapter 5: Conclusions

The effects of additives and milling on the densification and purification of zirconium diboride obtained from zirconia and boron oxide by magnesiothermic MASHS were studied using an induction heating system.

Experiments at 2000 °C successfully removed oxide impurities from ZrB_2, but the equipment was damaged. This led to exploring additives for reducing oxide impurities and sintering the sample at lower temperatures.

Boron carbide and molybdenum silicide were both successful in removing additives at a temperature of 1850 °C. However, sample densities drastically dropped after heating. Higher pressing forces led to higher densities prior to heating, but, even with high pressing forces and the use of boron carbide as an additive, the relative densities after heating were low (<42%).

Lastly, high-energy ball milling of powders was explored. Compositions without additives had adequate relative densities after pressing (60% for 1-min milling and 70% for 5-min milling), but they remained virtually the same after heating. In contrast, milled samples with boron carbide as an additive experienced an increase in density from 65% for a milling time of 1 min to 75% for a milling time of 5 min.

Summarizing, neither factor (milling, pressing, or adding boron carbide) taken alone was sufficient for promoting densification. A combination of all these factors is necessary for increasing density of ZrB_2 during the heating process.

References

[1] V. D Dhareppagol, A. Saurav "The Future Power Generation with MHD Generators", *International Journal of Advanced Electrical and Electronics Engineering,* vol.2, no. 6, p. 101-105, 2013.

[2] N. Kayukawa, "Open-Cycle Magnetohydrodynamic Electrical Power: A Review and Future Perspectives", *Progress in Energy and Combustion Science*, vol 30, p. 33-60,2004.

[3] G. Rudins, "U.S. and USSR MHD Electrode Materials Development", Rand, Santa Monica, Ca, 1974.

[4] V. K. Rihatgi, "High Temperature Materials for Magnetohydrodynamic Channels", *Bullletin of Materials Science*, vol. 6, no. 1, pp. 71-82, 1984.

[5] A. Bellosi, F. Monteverde, D. Sciti, "Fast densification of Ultra-High-Temperature Ceramics by Spark Plasma Sintering", The American Ceramic Society, vol.3, no. 1, pp. 32 – 40, 2006.

[6] S. Cordova and E. Shafirovich, " Toward a better conversion in magnesiothermic SHS of zirocnium diboride" *Journal of Material Science,* vol. 53, no. 19, pp. 13600-13616, 2018.

[7] M. Brochu, B.D Gauntt, L. Boyer, R.E. Loehman, "Pressureless reactive sintering of ZrB_2 ceramic" *Journal of the European Ceramic Society,* vol. 29, pp. 1493-1499, 2009.

[8] D. Sciti, F. Monteverde, S. Guicciardi, G. Pezzotti, A. Bellosi "Microstructural and mechanical properties of ZrB_2-$MoSi_2$ ceramic composites produced by different sitnering techniques", *Material Science and Engineering A,* vol. 434, pp. 303-309, 2006.

[9] A. Balbo and D. Sciti, "Spark Plasma Sintering and Hot Pressing of ZrB2-MoSi2 Ultra-High-Temperature Ceramics", *Materials Science and Engineering A,* vol. 475, pp. 108-112, 2008.

[10] S. Guo, T. Nishimura, Y Kagawa, J. Yang, "Spark Plasma Sintering of Zirconium Diborides", Journal of the American Ceramic Society, vol. 91, no. 9, pp. 2848-2855, 2008.

[11] W. G. Fahrenholtz, G. E. Hilmas, S. C. Zhang and S. Zhu, " Pressureless Sintering of Zirconium Diboride: Particle Size and Additive Effects", Journal of the American Ceramic Society, vol. 91, no. 5, p. 1398 -1404, 2008.

[12] S. C. Zhang, G. E. Hilmas and W. G. Fahrenholtz, "Pressureless Densification of Zirconium Diboride with Boron Carbide Additions", *Journal of the American Ceramic Society,* vol. 89, no. 5, pp. 1544-1550, 2006.

[13] A. L. Chamberlain, W. G. Fahrenholtz and G. E. Hilmas, "Pressureless Sintering of Zirconium Diboride", *Journal of the American Ceramic Society,* vol. 89, no. 2, pp. 450-456, 2006.

[14] L. Silvestroni and D. Sciti, "Effects of $MoSi_2$ Additions on the Properties of Hf- and Zr-B_2 Composites Produced by Pressureless Sintering", *Scripta Materialia* , vol. 57, pp. 165-168, 2007.

[15] G. P. Shveikin and A. L. Ivanovskii, "The Chemical Bonding and Electronic Properties of Metal Borides", *Russian Chemical Reviews*, vol. 63, no. 9, pp. 711-734, 1994.

[16] M. M. Opeka, I. G. Talmy, E. J. Wuchina, J. A. Zaykoski and S. J. Causey, "Mechanical, Thermal, and Oxidation Properties of Refractory Hafnium and Zirconium Compounds", *Journal of the European Ceramic Society*, vol. 19, p. 2405, 1999.

[17] W. G. Fahrenholtz and G. E. Hilmas, "Refractory Diborides of Zirconium and Hafnium", *Journal of the American Ceramic Society*, vol. 90, no. 5, pp. 1347-1364, 2007.

[18] A. Rezaie, W. G. Fahrenholtz and G. E. Hilmas, "Effect of Hot Pressing Time and Temperature on the Microstructure and Mechanical Properties of ZrB2-SiC", *Journal of Materials Sicence* , vol. 42, pp. 2735-2744, 2007.

[19] X.G, Wang, W,M Guo, Y. M. Kan, G.J. Zhang, " Hot-Pressed ZrB_2 Ceramics With Composite Additives of Zr and B_4C", *Advance Engineering Materiels*, vol. 12, no.9, pp 893-898, 2010.

[20] D. Pham, J. H. Dycus, J. M. LeBeau, V. R. Manga, K. Muralidharan and E. L. Corral, "Processing Low-Oxide ZrB_2 Ceramics with High Strength Using Boron Carbide and Spark Plasma Sintering", *Journal of The American Ceramic Society*, vol. 99, no. 8, pp. 2585-2592, 2016.

[21] S. C. Zhang, G. E. Hilmas and W. G. Farenholtz, "Pressureless Sintering of ZrB2-SiC Ceramics", *Journal of the American Ceramic Society*, vol. 91, no. 1, pp. 26-32, 2008.

[22] A. K. Khanra, L. C. Pathak, S. K. Mishra and M. M. Godkhindi, "Sintering of Ultrafine Ziconium Diboride Powder Prepared by Modifies SHS Technique", *Advances in Applied Ceramics*, vol. 104, no. 6, pp. 282-284, 2005.

Vita

Gabriel Llausas obtained his degree of Bachelor of Science in Mechanical Engineering from the University of Texas at El Paso in May 2017. During his undergraduate studies, he participated in research with the department of Civil Engineering at the University of Texas at El Paso. In summer 2017 he enrolled in the Master's Program in Mechanical Engineering and began studying pressureless sintering of zirconium diboride obtained by combustion synthesis. He presented results of his studies at the 2019 Annual Project Review Meeting for Crosscutting Research, Rare Earth Elements, Gasification and Transformative Power Generation, April 9-11, 2019, Pittsburgh, PA,